ACS OMEGA

http://pubs.acs.org/journal/acsodf

Article

Preparation and Characterization of Temperature/pH Dual-Responsive Gel Spheres for Immobilizing Nitro Bacteria

Qiong Wan, Xuan Li, Yingchun Ren, Yixi Cao, Kai Ju, Guohong Yang, Yongqing Sun, and Xinyan Zhang*

Cite This: *ACS Omega* 2022, 7, 5646−5656

Read Online

ACCESS | Metrics & More | Article Recommendations | Supporting Information

ABSTRACT: The temperature/pH dual-responsive gel spheres were prepared by orthogonal experiments and response surface methodology, and finally, the optimal synthesis conditions were obtained by a composite score, including swelling, mechanical properties, mass transfer properties, and so forth. The results showed that a sodium alginate concentration of 3% (w/v), $CaCl_2$ concentration of 2% (w/v), gelling time of 40 h, drop height of 14 cm, NaCl concentration of 0.6% (w/v), *N*-isopropylacrylamide concentration of 0.03% (w/v), and acrylic acid concentration of 4.06% (w/v) were optimal synthesis conditions. The environmental change tolerance experiments showed that the nitrogen removal of the dual-response nitrifying gel spheres was better than the domesticated sludge at low temperatures (4 °C) and in alkaline (pH 9 and 10) conditions. The as-obtained gel spheres can respond intelligently to the changes in ambient temperature and pH. It is hoped that this study will provide technical parameters for the development and application of microbial immobilization carriers.

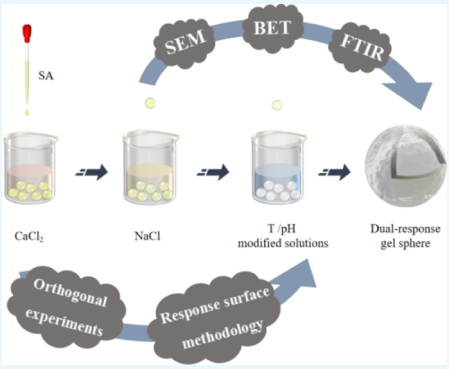

1. INTRODUCTION

Microbial immobilization is a vital way to enhance the functionality of microorganisms, where the target microorganisms are confined to a limited area (carrier material) to maintain high biomass and biological activity.[1] Compared to free bacteria, immobilized microorganisms have the advantages of high biodegradation rates, good environmental tolerance, and easy solid−liquid separation.[2] Simultaneously, the immobilization technology is suitable for various functional microorganisms, including anaerobic ammonia-oxidizing bacteria, aerobic denitrifying bacteria, and hydrocarbon-degrading bacteria.[3−6] Therefore, the technology has gradually shown great potential in different areas such as bio-hydrogen production, soil remediation, and wastewater treatment.[7−9]

The choice of the carrier material is crucial to the diffusion of microbial immobilization techniques. A good carrier material should have unique features, including good stability, high mass transfer capacity, cheap and easy raw materials availability, and good biocompatibility.[10,11] Particularly prominent among these is the natural organic carrier sodium alginate (SA), a linear anionic polysaccharide composed of *β*-D-mannuronic acid and *α*-*l*-guluronic acid.[12−14] It is enriched with −OH and −COOH, can form stable hydrogels with multivalent cations such as Ca^{2+} (except Mg^{2+} cations), and is currently one of the most demanded carrier materials.[15,16] Since the integrated adsorption—biodegradation—assimilation process is the only mechanism behind the removal of targeted pollutants by immobilized microorganisms,[2] changes in the external environment such as temperature, pH, magnetic field, ionic strength, and so forth can inhibit the growth and metabolism of free microorganisms, resulting in lower pollutant removal rates. Therefore, the development and promotion of gel spheres resistant to external environmental changes are highly recommended.

Poly-*N*-isopropyl acrylamide (PNIPAAm) and polyacrylic acid (PAA) are typical sensitive polymers utilized to prepare responsive gel spheres. PNIPAAm is thermally responsive due to its inherently lower critical solution temperature (LCST), approximately 32 °C.[17−19] This is demonstrated by the fact that when the ambient temperature is below LCST, PNIPAAm appears to swell hydrophilically, and conversely, it shrinks in volume and is hydrophobic.[20] PAA can respond to pH value changes by protonation or deprotonation due to the abundance of ionizable −COOH moieties in its structure.[21] Numerous papers have shown that gel spheres modified by PNIPAAm or PAA show a satisfactory response to temperature/pH changes, thus resisting the inhibition of functional microorganisms' activity by external environmental changes.[22−25]

Received: August 17, 2021
Accepted: January 26, 2022
Published: February 8, 2022

https://doi.org/10.1021/acsomega.1c04469
ACS Omega 2022, 7, 5646−5656

In this study, the optimum calcium alginate (CA) gel spheres were successfully prepared using orthogonal experiments; on this behalf, the pore structure was optimized by the modification effect of NaCl solution. The biocompatible CA gel spheres were used as the core substrate and interacted with NIPAAm, acrylic acid (AA), and *N*,*N*-methylenebisacrylamide (MBA) reagents to produce a temperature/pH responsive layer and result in the formation of optimizing environmentally dual-responsive gel spheres. It is proposed that this study will provide a new platform for the development and application of microbial immobilization carriers.

2. RESULTS AND DISCUSSION

2.1. Preparation and Optimization of CA Gel Spheres.

SA is the prime material required for the preparation of CA gel spheres, and its mass concentration affects the sphericity, mechanical strength, and ease of preparation of gel spheres. Lower concentration of SA results in poor sphericity and poor strength, while higher concentration of SA provides higher strength CA spheres due to its high viscosity, but it still suffers from severe trailing and complicated preparation. Besides, previous studies have suggested that $CaCl_2$ concentration, gel time, and drop height also have a dominant effect on CA gel sphere properties (such as sphericity, mechanical strength, and swelling).[26−28] Therefore, in this study, the above four factors were tested orthogonally to determine the optimal synthesis conditions for CA gel spheres, and the results are shown in Table 1. The relationship between factors and scores was also plotted using the value of each factor level as the horizontal coordinate and the mean value of the corresponding composite score for each factor level as the vertical coordinate (Figure 1). As depicted in Figure 1, the composite score of CA gel spheres tends to increase first and then decrease with increasing SA concentration, with a maximum value achieved at a SA concentration of 3% (w/v). Similarly, the CA gel spheres achieved a maximum composite score at a $CaCl_2$ concentration of 2% (w/v), a gelling time of 40 h, and a drop height of 14 cm. It was deduced that the optimal synthesis conditions for CA gel spheres are $A_4B_1C_4D_5$ (A_4, B_1, C_4, and D_5 indicate SA concentration of 3% (w/v), $CaCl_2$ concentration of 2% (w/v), gelling time of 40 h, and drop height of 14 cm, respectively). Based on the magnitude of the *R*-value of the extreme difference derived from the orthogonal experiment and the results of the ANOVA presented in Table 2, it could be seen that the ranking of the factors affecting the composite score was $A(20.4) > C(4.8) > B(4) = D(4)$. SA concentration significantly affected the composite score.

Table 1. Orthogonal Test Results[a]

	factors				
sample	*A* (%)	*B* (%)	*C* (h)	*D* (cm)	composite score
1	0.5	2	10	6	22
2	0.5	3	20	8	24
3	0.5	4	30	10	15
4	0.5	5	40	12	22
5	0.5	6	50	14	14
6	1	2	20	10	30
7	1	3	30	12	27
8	1	4	40	14	32
9	1	5	50	6	28
10	1	6	10	8	25
11	2	2	30	12	37
12	2	3	40	14	39
13	2	4	50	6	32
14	2	5	10	8	40
15	2	6	20	10	31
16	3	2	40	14	43
17	3	3	50	6	40
18	3	4	10	8	40
19	3	5	20	10	36
20	3	6	30	12	40
21	4	2	50	6	38
22	4	3	10	8	38
23	4	4	20	10	36
24	4	5	30	12	38
25	4	6	40	14	40

[a]Note: *A*, *B*, *C*, and *D* indicate SA concentration, $CaCl_2$ concentration, gelling time, and drop height, respectively.

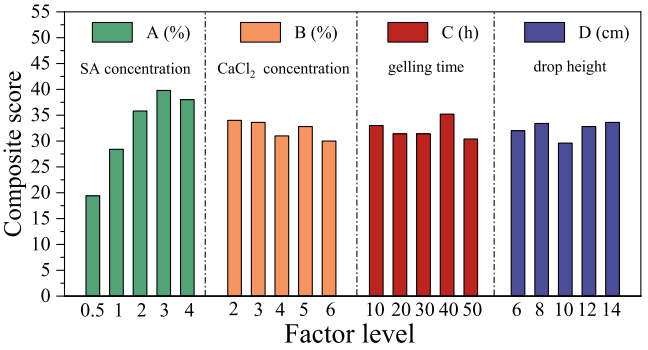

Figure 1. Relationship diagram between factors and score.

2.2. Preparation and Optimization of NaCl-Modified Gel Spheres.

High concentrations of Ca^{2+} ions can cause changes in the structure of the resulting CA gel spheres to make them too dense, which negatively impacts their mass transfer properties.[29] It has been shown that immersing CA gel spheres in a suitable concentration of NaCl solution can effectively improve this defect, and some of the chelated carboxylate moieties are replaced by Ca^{2+} to free state by Na^+, making the internal structure of the gel spheres more loose and porous.[30] In this study, the optimum CA gel spheres produced in Section 2.1 were placed in NaCl solutions of different concentrations (0−0.9%, w/v) and scored in four aspects: swelling, mechanical strength, oscillatory breakage rate, and mass transfer performance. As can be seen from the results presented in Figure 2, the highest composite score was achieved at 0.6% (w/v) NaCl-modified gel spheres. Therefore, 0.6% (w/v) NaCl solution was chosen as the optimal synthesis condition for the NaCl-modified gel spheres.

2.3. Preparation and Optimization of Temperature/pH Dual-Response Gel Spheres.

Response surface methodology (RSM) is one of the ideal methods to reduce the number of experiments and is used for modeling, data analysis, and optimization purposes.[31] Table 3 shows the results of the trials of the effect of the independent variables NIPAAm, MBA_1, AA, and MBA_2 concentration on the composite score. Figure 3 shows a response surface plot of the effect of the independent variables on the composite score. Figure 3a,c shows that NIPAAm concentration was inversely proportional to the composite score if MBA_1 concentration was certain. The predicted maximum composite score of 38.13 was achieved at

https://doi.org/10.1021/acsomega.1c04469
ACS Omega 2022, 7, 5646−5656

Table 2. Analysis of Variance and Significance Test[a]

source	sum of squares of deviations	freedom	mean square	*F*-value	$F_{0.05}$ (4,4)	$F_{0.01}$ (4,4)	significance
A	1413.04	4	353.26	23.93	6.39	15.98	**
B	59.04	4	14.76	1.00	6.39	15.98	
C	70.64	4	17.66	1.20	6.39	15.98	
D	52.64	4	13.16	0.89	6.39	15.98	
error	59.04	4	14.76				
sum	1654.4	20					

[a]Note: *A*, *B*, *C*, and *D* indicate SA concentration, $CaCl_2$ concentration, gelling time, and drop height, respectively, ** indicates highly significant correlation.

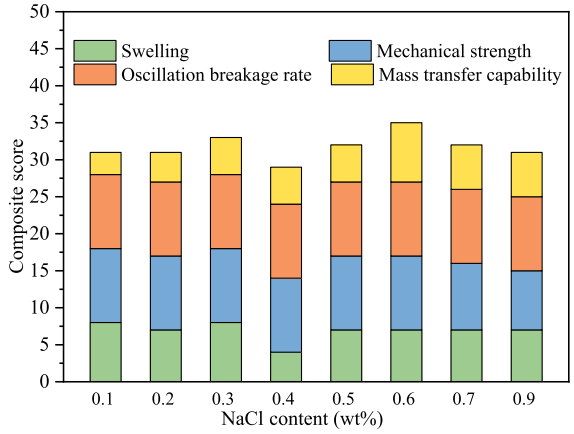

Figure 2. Relationship diagram between NaCl concentration and score.

NIPAAm and MBA_1 concentration of 0.03 and 0.02%, respectively. From Figure 3b,d, it could be seen that if the MBA_2 concentration was certain, the composite score tends to increase and then decrease with the increase of AA concentration. The maximum composite score of 38.13 was achieved at AA and MBA_2 concentration of 4.06 and 0.26%, respectively. Therefore, the optimal synthesis conditions for the dual-response gel spheres were selected as 0.03 and 0.02% of NIPAAm and MBA_1 in the temperature-modified solution, 4.06, and 0.26% of AA and MBA_2 in the pH-modified solution.

2.4. Gel Sphere Characterization. *2.4.1. SEM Analysis.* The optimum CA gel spheres, NaCl-modified gel spheres, and dual-response gel spheres were not significantly different, all being spheres of uniform particle size (approximately 4 mm in diameter) and opalescent and translucent throughout. After dehydration-liquid nitrogen-freeze dried operations, all types of gel spheres had exhibited an undulating surface (Figure 4a−c) and a complete network structure (Figure 4d−f). The surface of the optimum CA gel spheres modified by NaCl and dual response, in turn, showed a trend of greater fold (Figure 4a), insignificant fold (Figure 4b), greater, uniform, and lesser fold (Figure 4c). This phenomenon may be related to the pore distribution and structure of the various types of gel spheres. From the monitored profile, it can be stated that the NaCl-modified gel spheres (Figure 4e) showed evident delamination from the outside to the inside compared to the optimum CA gel spheres (Figure 4d), and this phenomenon may be related to the length of the NaCl modification time. Meanwhile, the shell−core structure (dense outside and sparse inside) shown in Figure 4f confirms the successful development of optimal dual-response gel spheres, forming a composite gel sphere with a CA as the core and a temperature/pH responsive layer as the shell layer. Besides, this structure effectively traps the microorganisms embedded in the gel spheres, providing sufficient space for them to grow and multiply. Moreover, it can provide a stable living environment for the proper growth of microorganisms. When the temperature/pH of the environment fluctuates, the outer temperature/pH response layer can achieve a real-time response and maintain a relatively stable and favorable microenvironment for microorganisms to grow.

Table 3. Box-Behnken Design and Effect of Independent Variables on Composite Score as a Response

runs	NIPAAm (%)	MBA_1 (%)	AA (%)	MBA_2 (%)	composite score
1	0.93	0.01	0.1	0.23	28
2	1.83	0.02	5	0.23	36
3	0.93	0.02	2.55	0.23	37
4	0.93	0.03	2.55	0.01	36
5	0.03	0.02	0.1	0.23	29
6	0.93	0.02	2.55	0.23	37
7	0.93	0.01	2.55	0.45	35
8	0.03	0.01	2.55	0.23	37
9	0.93	0.02	0.1	0.01	28
10	0.93	0.02	2.55	0.23	37
11	0.93	0.02	5	0.45	36
12	1.83	0.02	2.55	0.01	34
13	1.83	0.02	2.55	0.45	36
14	0.93	0.03	5	0.23	35
15	0.03	0.02	5	0.23	37
16	1.83	0.01	2.55	0.23	36
17	0.93	0.02	2.55	0.23	37
18	0.93	0.03	2.55	0.45	37
19	0.93	0.02	2.55	0.23	36
20	0.93	0.03	0.1	0.23	29
21	0.03	0.03	2.55	0.23	36
22	0.03	0.02	2.55	0.01	36
23	1.83	0.03	2.55	0.23	35
24	0.93	0.01	2.55	0.01	33
25	0.03	0.02	2.55	0.45	35
26	0.93	0.02	0.1	0.45	31
27	1.83	0.02	0.1	0.23	33
28	0.93	0.02	5	0.01	32
29	0.93	0.01	5	0.23	37

2.4.2. BET Analysis. From the summary table of gel sphere properties (Table 4), it could be observed that the average particle size of the three optimum gel spheres was 3.8 mm, and there was no significant difference found in density (all close to the density of water). Regarding specific surface area and pore size, the optimum CA gel spheres had a significant specific surface area value of 1.455 m^2/g with an average pore size of 15.10 nm. The specific surface area of the optimum NaCl-modified gel spheres decreased abruptly up to 0.052 m^2/g, probably due to the full replacement of Ca^{2+} in the CA gel

https://doi.org/10.1021/acsomega.1c04469
ACS Omega 2022, 7, 5646−5656

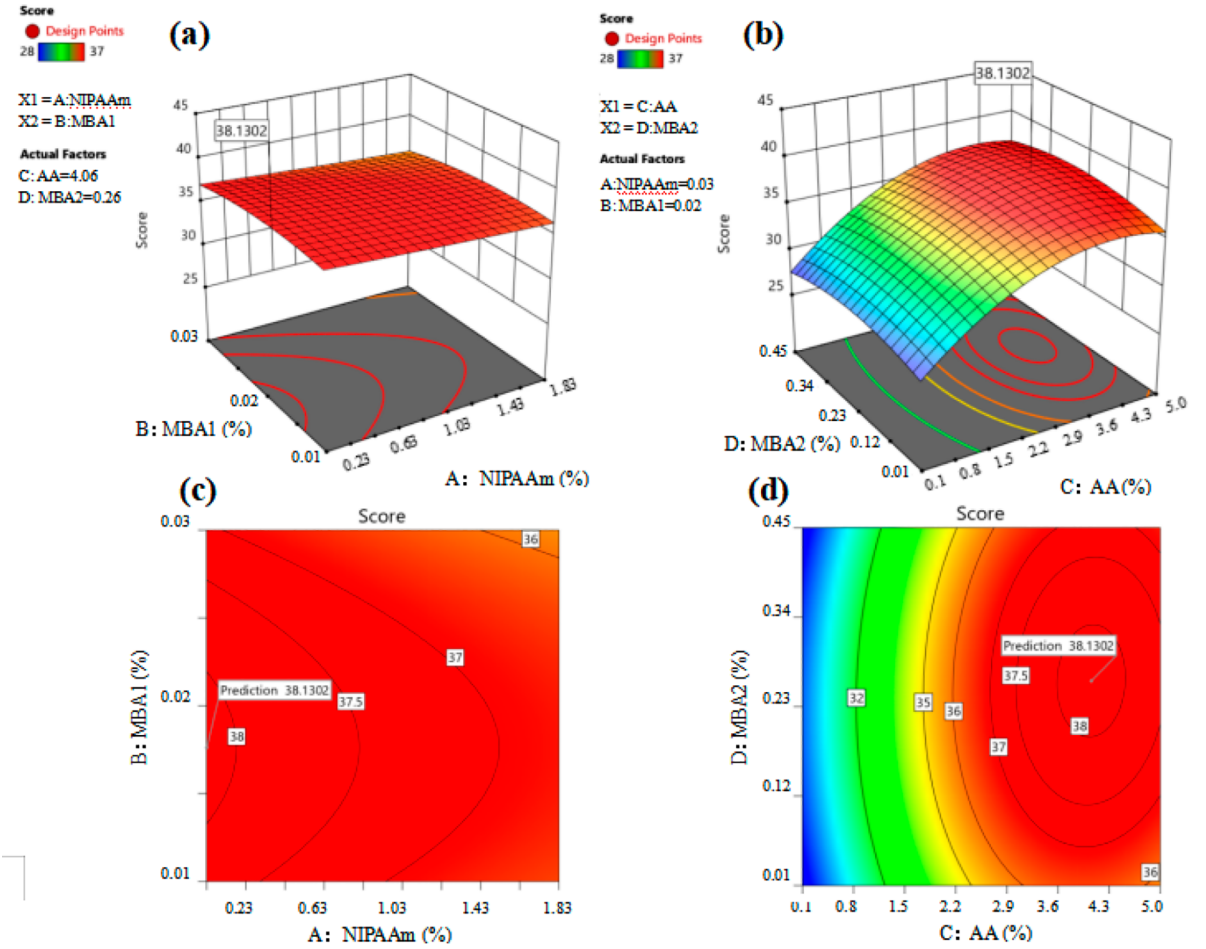

Figure 3. Surface plot for composite score with respect to the three-dimension (3D) of NIPAAm and MBA_1(a); 3D of AA and MBA_2(b); 2D of NIPAAm and MBA_1(c); and 2D of AA and MBA_2(d).

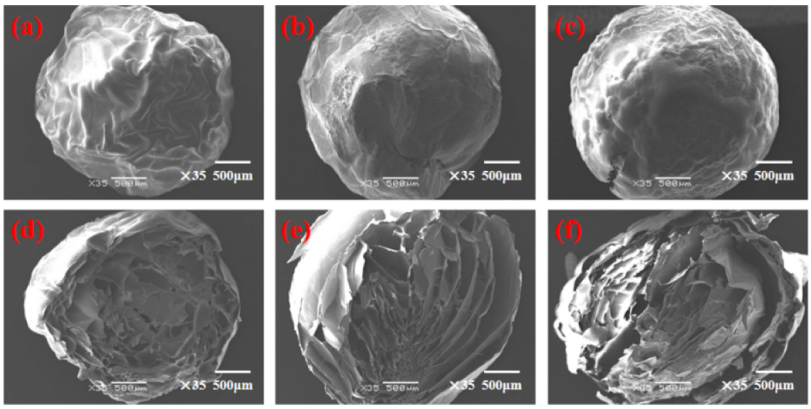

Figure 4. SEM surface image of the optimum CA gel spheres (a), NaCl-modified gel spheres (b), and dual-response gel spheres (c); SEM interior image of the optimum CA gel spheres (d), NaCl-modified gel spheres (e), and dual-response gel spheres (f).

spheres by Na^+, resulting in a lower cross-link density and increased macropore content (average pore size of 62.10 nm).[30] The optimum dual-response gel spheres were based on the optimum NaCl-modified gel spheres modified with polymers PNIPAAm and PAA, whose 3D network structure intertwines with the CA gel spheres, a 3D grid structure, and formed a temperature/pH responsive layer on the surface.[32] The final mesoporous material with a specific surface area of 0.113 m^2/g and an average pore size of 26.88 nm was produced.

2.4.3. FT-IR Analysis. The optimum CA gel spheres (Figure S1a) and the optimum NaCl modified gel spheres (Figure S1 b) showed the same trend in infrared (IR) spectra, both having −OH stretching vibration peaks (positioned at 3339 cm^{-1}), $-COO^-$ antisymmetric (located at 1592 cm^{-1}), and symmetric (peaked at 1416 cm^{-1}) stretching vibration peaks.[33,34] However, the latter individual characteristic peaks

https://doi.org/10.1021/acsomega.1c04469
ACS Omega 2022, 7, 5646−5656

Table 4. Summary of the Three Types of Gel Sphere Properties

type	diameter mm	density g/cm^3	BET specific surface area m^2/g	average pore size nm
the optimum CA gel spheres	3.8	0.98	1.455	15.10
the optimum NaCl-modified gel spheres		1.00	0.052	62.10
the optimum dual-response gel spheres		0.99	0.113	26.88

emerged with greater intensity and were more pronounced, indicating that the arrangement of the functional groups was sparser after modification with NaCl. Compared to Figure S1b, a broad peak detected at 3398 cm^{-1} was assigned to N−H conjugation, peak monitored at 1243 cm^{-1} was referred to C−N bond stretching vibration, isopropyl C−H bond out-of-plane wobble vibration at 672 cm^{-1}, and C═O stretching vibration at 1719 cm^{-1} (characteristic peaks of carboxyl groups) in Figure S1c, all endorsed the successful preparation of the optimum dual-response gel spheres.

2.5. Gel Sphere Response Experiment. Figure 5 exhibits the variations in swelling for three types of optimum gel spheres (made in Sections 2.1−2.3, respectively) for different temperatures 5−50 °C (at pH 7) or different pH 2−12 (at temperature 20 °C). In Figure 5a, it could be seen that the swelling of the three types of optimum gel spheres tends to increase first and then decrease with the increase in temperature, and the maximum swelling is achieved at 30 °C. The optimum dual-response gel spheres swelling increased for the temperature range 5−30 °C, probably due to the increased hydration of the gel sphere network at higher temperatures.[35] As in numerous previous studies, the dual-response gel spheres did not achieve high swelling at high temperatures (40−50 °C).[36] This may be due to the fact that under high temperature conditions, the intramolecular hydrogen bonds were broken, the hydrophobicity of the gel spheres was increased, and the water molecules within the structure were released, reducing the degree of swelling.[37,38] The optimum NaCl-modified gel spheres had significantly lower mechanical properties (6−9 N) compared to the optimum CA gel spheres (>20 N), although they had a large swelling at all temperatures. The optimum dual-response gel spheres were temperature-sensitive and had a high mechanical strength (11−14 N), making them more beneficial for encapsulating microorganisms for biological treatment of wastewater.

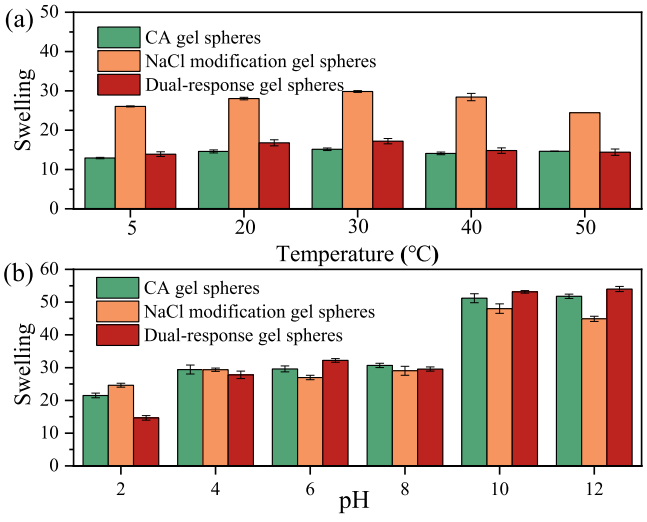

Figure 5. Effect of response on the swelling of gel spheres: (a) temperature and (b) pH.

Figure 5b shows that the swelling of the three types of gel spheres increased with an increase in the pH value. The change in swelling was relatively flat for the pH range 2−8 and 10−12 and increased significantly for the pH range 8−10. At pH 10, the swelling of the optimum CA gel spheres, the optimum NaCl-modified gel spheres, and the optimum dual-response gel spheres increased to 51.19, 48.01, and 53.14%, respectively. Overall, a minimum of 14.67% (at pH 2) and maximum of 53.99% (at pH 12) swelling of the gel spheres occurred on the dual-response gel spheres, achieving a dual-response gel sphere response characteristic to pH. This was closely related to the formation of a −COOH− rich temperature/pH-responsive layer on its surface (consistent with the results in Figure S1c). Moreover, −COOH was negatively charged (−COO$^-$) at higher pH due to deprotonation, with an increase in electrostatic repulsion, changes in the pore structure of the gel spheres, and a consequent increase in swelling monitored.[21,39,40]

Figure 6 shows that the morphology of the optimum dual-response gel spheres at different temperatures and pH conditions. At the same temperature (T = 5 °C), the higher the pH, the larger the size of the gel spheres (increasing by about 0.8 mm). Similarly, at the same pH (pH = 10), the higher the T, the larger the size of the gel spheres (increasing by about 0.7 mm).

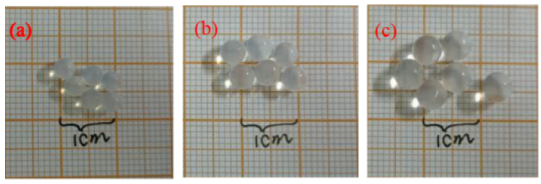

Figure 6. Morphology of dual-response gel spheres: (a) T = 5 °C, pH = 7; (b) T = 5 °C, pH = 10; and (c) T = 30 °C, pH = 10.

2.6. Environmental Change Tolerance Experiment. Figure 7 exhibits denitrification performance of the optimum dual-response nitrifying bacteria gel spheres for different temperatures 4−50 °C (at pH 7) or pH 4−10 (at temperature 20 °C). The NH_4^+−N removal rate by the optimum dual-response nitrifying bacteria gel spheres increased first and then decreased with increasing temperature (Figure 7a). The maximum NH_4^+−N removal rate (45.21%) was achieved at 30 °C. The reason may be that the gel spheres had a temperature/pH responsive layer, when the temperature was lower than LCST, the gel spheres appear to swell hydrophilically and the surface micropores open up, allowing the nitrobacteria embedded in the inner layer of the gel spheres to come into full contact with the NH_4^+−N in solution.[37] However, compared to domesticated sludge, it did not show nitrogen removal advantages at medium temperatures (20 and 30 °C) due to mass transfer limitations. In contrast, the optimum dual-response nitrifying bacteria gel spheres showed superior denitrification performance at low temperatures (4 °C) with 31.07% removal of NH_4^+−N, 6.87% higher than the domesticated sludge. The reason may be that the gel slowed

https://doi.org/10.1021/acsomega.1c04469
ACS Omega 2022, 7, 5646−5656

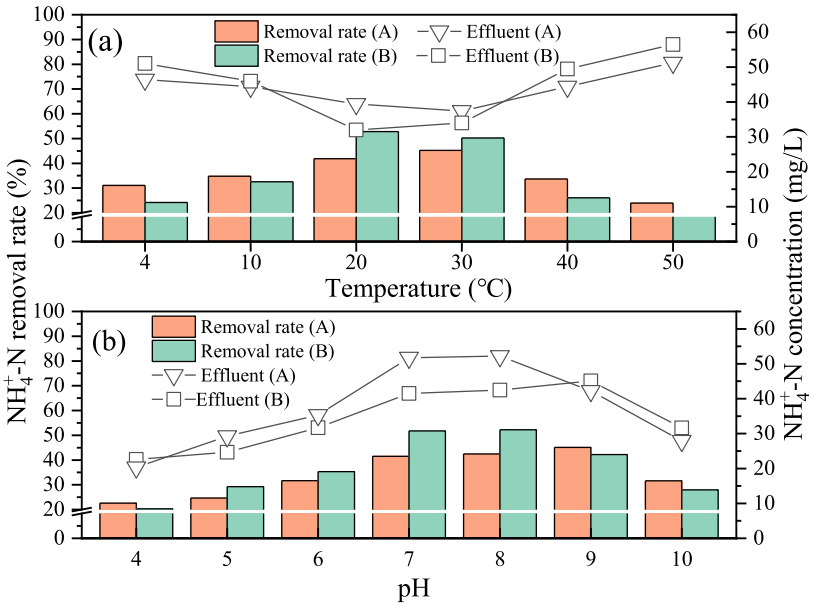

Figure 7. Tolerance to environmental changes of the optimum dual-response nitrifying bacteria gel spheres (A) and acclimated sludge (B): (a) temperature and (b) pH.

down the inhibition of microbial growth at low temperatures and provided a good living space for microorganisms, thus offering the possibility of effective degradation of ammonia nitrogen.[14,41,42]

Overall, the effect of pH on the domesticated sludge and the optimum dual-response nitrifying bacteria gel spheres showed similar trends: NH_4^+−N removal rate increased and then decreased with increasing pH (Figure 7b). Due to the intrinsic characteristics of the nitrifying bacteria [optimum pH range for AOB and NOB (7.5−8.5),[43] the maximum NH_4^+−N removal rate (52.21%) was achieved at pH 8 for the domesticated sludge. The optimum dual-response nitrifying bacteria gel spheres did not show nitrogen removal benefits at this pH due to mass transfer limitations. On the contrary, at pH 9 and 10, there was a high ammonia removal (45.10 and 31.63%, respectively), which was 2.89 and 3.69% higher than that of the domesticated sludge, respectively. The reason was that at high pH, the pore structure of the optimum dual-response nitrifying bacteria gel spheres changes, with a more porous and sparse surface and increased removal of ammonia nitrogen.[39]

In summary, the optimum dual-response gel spheres had the ability to enhance the tolerance of microorganisms to unfavorable external environments and was expected to provide a reference for developing and applying microbial immobilization carriers.

3. CONCLUSIONS

In the study, we explored the optimal synthesis conditions for the dual-response gel spheres. The main conclusions can be summed up as follows

(1) By constructing an orthogonal experiment with the composite score as the evaluation index, it was concluded that the optimum synthesis conditions for CA gel spheres were SA concentration of 3% (w/v), $CaCl_2$ concentration of 2% (w/v), gelling time of 40 h, and drop height of 14 cm. In addition, the factors affecting the composite score of the gel spheres were ranked as follows: SA concentration > gelling time > $CaCl_2$ concentration = drop height.

(2) The swelling and mass transfer properties of the CA gel spheres modified with 0.6% (w/v) NaCl were significantly improved than those of the pristine CA gel spheres.

(3) The optimal synthesis conditions for the dual-response gel spheres were explored using the RSM: NIPAAm, MBA_1, AA, and MBA_2 concentrations of 0.03% (w/v), 0.02% (w/v), 4.06% (w/v), and 0.26% (w/v), respectively.

(4) The results of the environmental change tolerance experiment, the response experiment, and various characterization methods (SEM, BET, and FT-IR) showed that the optimum temperature/pH dual-response gel spheres were successfully prepared. It is hoped that it will provide a valuable reference for the development and application of microbial immobilization carriers, and consideration can be given to exploring the implementation of LCST and pH control of the material in the future.

4. MATERIALS AND METHODS

4.1. Reagents and Instruments. SA(AR), $CaCl_2$(AR), NaCl(AR), ammonium persulfate (APS) (AR), and tetramethylethylenediamine (TMEDA) (BR) were purchased from Sinopharm Chemical Reagent Co. MBA(AR) was purchased from Sas Chemical Technology (Shanghai) Co. NIPAAm(BR) and AA(BR) were purchased from Tricia (Shanghai) Chemical Industry Development Co. Sodium bisulfite (SBS) (ACS) was purchased from Beijing Bailingway Technology Co.

A digital push−pull meter (HP-50, HANDPI, China) was used to measure the mechanical strength of the gel spheres. The structure and specific surface area of the gel spheres were observed and analyzed by using scanning electron microscopy (SEM) (JSM-6460LV, JEOL, Japan) and a specific surface and porosimetry instrument (ASAP 2020, Micromertics, USA), respectively. The changes in the gel spheres' characteristic

https://doi.org/10.1021/acsomega.1c04469
ACS Omega 2022, 7, 5646−5656

peaks after modification were analyzed by Fourier transform IR (FTIR) (Nicolet 6700, Thermo Scientific, USA) to cross-check the changes noticed in the material structure.

4.2. Preparation of Gel Spheres. The overall process of preparing the gel spheres is presented in Figure 8. The specific steps are as follows:

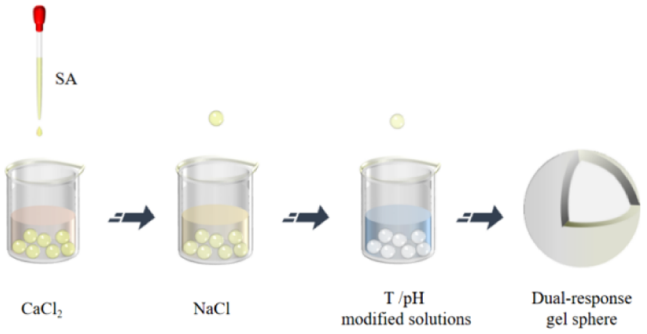

Figure 8. Preparation of gel spheres.

4.2.1. CA Gel Spheres. The SA solution was first cooled to room temperature after complete dissolution (50−60 °C water bath) and then added drop by drop to the $CaCl_2$ solution at a fixed height using a rubber-tipped dropper. It was cross-linked at 4 °C for a specific time and rinsed 2−3 times with deionized water. To obtain the optimum CA gel spheres, a 4-factor [A: SA concentration (%), B: $CaCl_2$ concentration (%), C: gelling time (h), and D: drop height (h)] 5-level orthogonal experiment was used in this study. The ultimate use of the gel spheres is to encapsulate microorganisms for the biological treatment of wastewater. As there is no unified evaluation standard, in order to evaluate the gel spheres quantitatively, a preliminary study was conducted by equally assigning weights to five aspects (sphericity,[33,44,45] swelling,[46−48] mechanical properties,[49−51] oscillatory breakage rate,[44,52,53] and mass transfer properties[42,44,54]) on the basis of previous studies by other scholars (Table 5). The orthogonal experimental design factors and scoring criteria are given in Tables 6 and 7.

4.2.2. NaCl-Modified CA Gel Spheres. The optimum CA gel spheres were cast into different concentrations (0−0.9%) of NaCl solution, left to react for 2 h, and rinsed 2−3 times with deionized water to obtain the optimum NaCl-modified CA gel spheres.

Table 6. Orthogonal Experimental Table

	factors[a]			
levels	*A* (%)	*B* (%)	*C* (h)	*D* (cm)
1	0.5	2	10	6
2	1	3	20	8
3	2	4	30	10
4	3	5	40	12
5	4	6	50	14

[a]Note: *A*, *B*, *C*, and *D* indicate SA concentration, $CaCl_2$ concentration, gelling time, and drop height, respectively.

Table 7. Gel Spheres Scoring Criteria

performance		score
sphericity	90−100% uniformly spherical in size (diameter = 4 mm), 0−20% adhesion	9−10
	50−90% uniformly spherical in size (diameter = 4 mm), the rest is ellipsoidal and olive shapes, 0−20% adhesion	5−8
	more than 50% non-spherical, heavily (more than 50%) adherent	0−4
swelling	swelling of 15−30	9−10
	swelling of 5−15 and 30−40	5−8
	swelling of 0−5 or >40	0−4
mechanical properties	mechanical strength of 20−25 N	9−10
	mechanical strength of 10−20 N	5−8
	mechanical strength of 0−1 N	0−4
oscillatory breakage rate	breakage rate of 0−10%	9−10
	breakage rate of 10−50%	5−8
	breakage rate >50%	0−4
mass transfer properties	actual nitrite nitrogen concentration/theoretical nitrite nitrogen concentration in gel spheres of 90−100%	9−10
	actual nitrite nitrogen concentration/theoretical nitrite nitrogen concentration in gel spheres of 70−90%	5−8
	actual nitrite nitrogen concentration/theoretical nitrite nitrogen concentration in gel spheres <70%	0−4

Table 5. Summary of Gel Sphere Performance

carrier	performance	remarks	references
PVA−SA	sphericity	scored for sphericity, size, and shape	44
CA		shape characterization of hydrogels using spherical factors	33
CA		SA concentrations were selected based on whether spherical and uniformly sized CA gel spheres were produced	45
SA/PEI	swelling	characterization using the swelling rate	46
semi-IPN superabsorbent nanocomposite			47
PVA/alginate			48
PAC−SA	mechanical properties	characterization using compressive strength	49
3D PVA gel beads			50
methyl cellulose/CA beads			51
PVA/SA	oscillatory breakage rate	agitation of gel beads at 600 rpm and final recording of the breakage rate	52
PVA/PPG hydrogel		agitation of gel beads at 2000 rpm and final recording of the breakage rate	53
PVA−SA		the pellets were placed in an isometric shaker for 48 h and the breakage was recorded	44
PVA−SA−diatomite	mass transfer properties	characterization using mass transfer rates	42
PAC−SA			54
PVA−SA		the gel spheres were immersed in ink for 20 min and characterized by the color shade of the central section and the radius of immersion	44

https://doi.org/10.1021/acsomega.1c04469
ACS Omega 2022, 7, 5646−5656

4.2.3. Temperature/pH Dual-Response Gel Spheres. 5 g of drained optimized NaCl-modified CA gel spheres was cast into the temperature-modified solution [a mixture(15 mL) of NIPAAm, MBA, APS (6.0 mg), and TMEDA (17.0 μL)], left to react for 2 h, and rinsed 2−3 times with deionized water to produce temperature-responsive gel spheres. It was continued to be cast into a pH-modified solution [a mixture (10 mL) of AA, MBA, APS (6.0 mg), and SBS (6.0 mg)], left to react for 30 min, and rinsed 2−3 times with deionized water to finally produce a temperature/pH dual-response gel sphere. Design-expert 8.0.5 software with the Box-Behnken RSM was used to determine the relationship between the variables and the responses. NIPAAm (X_1), MBA_1 (X_2), AA (X_3), and MBA_2 (X_4) concentrations were used as independent variables and the composite score (including swelling, mechanical properties, oscillatory breakage rate, and mass transfer properties) as the dependent variable to finally obtain the optimum temperature/pH dual-response gel spheres. The levels and ranges of the experimental independent variables are given in Table 8. Here, MBA_1 and MBA_2 were the cross linker MBA added to the temperature-modified solution and the pH-modified solution, respectively.

Table 8. Design Factor Level Table

			factor coding level		
number	variables	unit	−1	0	1
X_1	NIPAAm	(%)	0.03	0.93	1.83
X_2	MBA_1		0.01	0.02	0.03
X_3	AA		0.1	2.55	5
X_4	MBA_2		0.01	0.23	0.45

4.2.4. Optimum Dual-Response Nitrification Gel Spheres. The sludge (from the aeration tank of a university wastewater plant in Xi'an), which had been domesticated for 23 days, was made into a bacterial suspension (100 g/L) by centrifugation (2000 rpm, 10 min). The mixture was added to the SA solution in a certain ratio ($V_{SA}/V_{\text{bacteria suspension}}$ = 4:1) and mixed well. The subsequent preparation steps were the same as those for the final preferred optimum dual-response gel spheres.

4.3. Performance Characterization. *4.3.1. Swelling.* 20 dried gel spheres of uniform particle size were immersed in a 0.9% NaCl solution and left to swell at 25 °C until equilibrium reached, at which point the gel sphere mass (W_e) was constant. The formula is as follows

$$\text{swelling} = \frac{W_e - W_d}{W_d} \times 100\% \quad (1)$$

where W_e is the weight of gel sphere after swelling equilibrium in g; W_d is the weight of gel spheres after vacuum drying in g.

4.3.2. Mechanical properties. A digital push−pull gauge was used to measure the maximum pressure borne by the gel spheres. A uniform size gel sphere was placed on the lower platen, and the handwheel was shaken to move the upper platen downwards until the gel sphere was broken, and then the pressure was recorded at this point. The average of the three measurements was the maximum pressure to which the gel sphere was subjected.

4.3.3. Oscillatory breakage rate. 50 intact gel spheres were placed in equal amounts of 0.9% NaCl solution (30 mL), then put in a shaking incubator, and shaken at a constant temperature (25 °C) at an equal frequency (200 rpm for 3 days). The gel spheres were observed under a light microscope, and the breakage was analyzed. The formula for oscillatory breakage rate is as follows:

$$\text{oscillatory breakage rate} = \frac{S_0 - S_1}{S_0} \times 100\% \quad (2)$$

where S_0 is number of unbroken gel spheres before oscillation = 50; S_1 is number of unbroken gel spheres after oscillation.

4.3.4. Mass Transfer Properties. 10 g gel spheres were added to 20 mL of nitrite solution (10 mg/L), placed in an incubator, and shaken at constant temperature (25 °C) and at equal frequency (200 rpm) for 2 h. The concentration of nitrite in the solution was measured by the formula given below

$$\text{mass transfer properties} = \frac{(V_1 \times C_1 - V_1 \times C_2)/V_2}{V_1 \times C_1/(V_1 + V_2)} \times 100\% \quad (3)$$

where V_1 is initial nitrite nitrogen solution volume, 20 mL; V_2 is total volume of gel spheres dosed, 10 mL; C_1 is initial nitrite nitrogen solution concentration, 10 mg/L; and C_2 is nitrite nitrogen solution concentration after 2 h, mg/L.

4.3.5. SEM analysis. The gel spheres were dehydrated in a graded ethanol series [10 min in each of 20, 40, 50, 60, 70, 80, 90% (w/v) ethanol and then twice in anhydrous ethanol to remove the final traces of water]. The dehydrated beads were then placed in liquid nitrogen (5 min)—freeze dried (24 h) to obtain dry gel sphere particles. It was then cut in half with a knife, sprayed with gold, and placed on a conductive gel, and the surface structure and profile of the gel sphere were observed using SEM with a secondary electron detector, a scanning voltage of 20 kv, and a working distance of 7.0 mm.

4.3.6. BET analysis. The gel spheres were first treated with liquid nitrogen (5 min)—freeze dried (24 h) and then ground and sieved (80 mesh) to obtain the final dried gel sphere powder. 0.2 g was put into an ASAP-2020 pore structure surface area analyzer, and the sample was tested by a N_2 adsorption−desorption technique. The Brunauer−Emmett−Teller (BET) equation was used to calculate the specific surface area of the sample, and the BJH model was used for pore size analysis.

4.3.7. FTIR Analysis. FTIR spectra were recorded in the wavenumber range of 400−4000 cm using the KBr pellet method.

4.4. Temperature/pH Response Experiments. Three types of optimum gel spheres (optimum CA gel spheres, optimum NaCl modified gel spheres, and optimum dual-response gel spheres) were investigated for swelling. Thirty vacuum-dried spheres of the three optimum gel types were put into solutions of different temperatures (5, 20, 30, 40, and 50 °C) or pH (2, 4, 6, 8, 10, and 12) to investigate the variation of swelling with temperature and pH, respectively. The temperature values of the dispersions were adjusted with a refrigerator and a water bath thermostatic oscillator. The pH values were adjusted with a 0.1 M HCl solution and a 0.1 M NaOH solution.

4.5. Environmental Change Tolerance Experiment. The optimum dual-response nitrifying bacteria gel spheres (20% dosing rate) after three days of activation and the domesticated sludge with the same amount of bacteria were

https://doi.org/10.1021/acsomega.1c04469
ACS Omega 2022, 7, 5646−5656

put into the synthetic wastewater (Table 9 for specific components) at different temperatures (4−50 °C) or pH

Table 9. Composition of Synthetic Wastewater

components		concentration (mg/L)
NH4+−N	50	
$NaHCO_3$	600	
trace elements (0.25 mL/L)	$ZnSO_4·7H_2O$	0.11
	$Na_2MoO_4·2H_2O$	0.11
	$CoCl_2·6H_2O$	0.12
	$MnSO_4·H_2O$	0.117
	$NiCl_2·6H_2O$	0.104
	Na_2HPO_4	0.57
	$FeCl_3·6H_2O$	0.124

(4−10). Ammonia removal rate within 5 h was used as a performance indicator to assess tolerance to external environmental changes.

■ ASSOCIATED CONTENT

Supporting Information

The Supporting Information is available free of charge at https://pubs.acs.org/doi/10.1021/acsomega.1c04469.

FT-IR spectra of the gel spheres (PDF)

■ AUTHOR INFORMATION

Corresponding Author

Xinyan Zhang − *School of Architecture and Civil Engineering, Xi'an University of Science and Technology, Xi'an 710054, China*; Email: xyzhang2020@xust.edu.cn

Authors

Qiong Wan − *School of Architecture and Civil Engineering, Xi'an University of Science and Technology, Xi'an 710054, China*

Xuan Li − *School of Architecture and Civil Engineering, Xi'an University of Science and Technology, Xi'an 710054, China*; orcid.org/0000-0001-8715-9935

Yingchun Ren − *Yihai Kerry (Zhoukou) Biotechnology Co., Ltd., Zhoukou 466000, China*

Yixi Cao − *Shaanxi Water Affair Water Ecology Comprehensive Development Group Co., Ltd., Xi 'an 710075, China*

Kai Ju − *School of Architecture and Civil Engineering, Xi'an University of Science and Technology, Xi'an 710054, China*

Guohong Yang − *School of Architecture and Civil Engineering, Xi'an University of Science and Technology, Xi'an 710054, China*

Yongqing Sun − *School of Architecture and Civil Engineering, Xi'an University of Science and Technology, Xi'an 710054, China*

Complete contact information is available at: https://pubs.acs.org/10.1021/acsomega.1c04469

Author Contributions

Conceptualization, Q.W. Methodology, X.Y.Z.; Software, Y.Q.S.; Validation, X.Y.Z.; Investigation, Q.W.; Data Curation, K.J. and Y.X.C.; Writing-Original Draft Preparation, Q.W., X.L., and Y.C.R.; Writing-Review & Editing, K.J. and G.H.Y.

Notes

The authors declare no competing financial interest.

■ ACKNOWLEDGMENTS

This work was supported by the open fund of State Key Laboratory of Pollution Control and Resource Reuse (grant no. PCRRF18014), Shaanxi Provincial Education Department Research and Innovation Project Fund (grant no. 20JK0768), National Key R&D Program Specialized "Integrated Technology and Application Demonstration of Rural Water Supply and Drainage in Typical Water-Deficit Areas in the West" (grant no. 2016YFC0400703-3), Incubation fund of Xi'an University of Science and Technology (grant no. 201724), and the PhD start-up fund of Xi'an university of science and technology (grant no. 2018QDJ005).

■ REFERENCES

(1) Żur, J.; Wojcieszyńska, D.; Guzik, U. Metabolic Responses of Bacterial Cells to Immobilization. *Molecules* **2016**, *21*, 958.

(2) Das, M.; Adholeya, A. Potential uses of immobilized bacteria, fungi, algae, and their aggregates for treatment of organic and inorganic pollutants in wastewater. In Water challenges and solutions on a global scale. *ACS Symp. Ser.* **2015**, *1206*, 319−337.

(3) Wang, J.; Liang, J.; Sun, L.; Li, G.; Temmink, H.; Rijnaarts, H. H. M. Granule-based immobilization and activity enhancement of anammox biomass via PVA/CS and PVA/CS/Fe gel beads. *Bioresour. Technol.* **2020**, *309*, 123448.

(4) Ma, F.; Sun, Y.; Li, A.; Zhang, X.; Yang, J. Activation of accumulated nitrite reduction by immobilized Pseudomonas stutzeri T13 during aerobic denitrification. *Bioresour. Technol.* **2015**, *187*, 30−36.

(5) Cunningham, C. J.; Ivshina, I. B.; Lozinsky, V. I.; Kuyukina, M. S.; Philp, J. C. Bioremediation of diesel-contaminated soil by microorganisms immobilized in polyvinylalcohol. *Int. Biodeterior. Biodegrad.* **2004**, *54*, 167−174.

(6) Bouabidi, Z. B.; El-Naas, M. H.; Zhang, Z. Immobilization of microbial cells for the biotreatment of wastewater: a review. *Environ. Chem. Lett.* **2019**, *17*, 241−257.

(7) Kumar, G.; Mudhoo, A.; Sivagurunathan, P.; Nagarajan, D.; Ghimire, A.; Lay, C.-H.; Lin, C.-Y.; Lee, D.-J.; Chang, J.-S. Recent insights into the cell immobilization technology applied for dark fermentative hydrogen production. *Bioresour. Technol.* **2016**, *219*, 725−737.

(8) Tao, K.; Zhang, X.; Chen, X.; Liu, X.; Hu, X.; Yuan, X. Response of soil bacterial community to bioaugmentation with a plant residue-immobilized bacterial consortium for crude oil removal. *Chemosphere* **2019**, *222*, 831−838.

(9) Bilal, M.; Iqbal, M.; Hu, H.; Zhang, X. Mutagenicity and cytotoxicity assessment of biodegraded textile effluent by Ca-alginate encapsulated manganese peroxidase. *Biochem. Eng. J.* **2016**, *109*, 153−161.

(10) Dzionek, A.; Wojcieszyńska, D.; Guzik, U. Natural carriers in bioremediation: A review. *Electron. J. Biotechnol.* **2016**, *23*, 28−36.

(11) Nwankwegu, A. S.; Onwosi, C. O. Microbial cell immobilization: a renaissance to bioaugmentation inadequacies. A review. *Environ. Technol. Rev.* **2017**, *6*, 186−198.

(12) Bediako, J. K.; Lin, S.; Sarkar, A. K.; Zhao, Y.; Choi, J.-W.; Song, M.-H.; Wei, W.; Reddy, D. H. K.; Cho, C.-W.; Yun, Y.-S. Benignly-fabricated crosslinked polyethylenimine/calcium-alginate fibers as high-performance adsorbents for effective recovery of gold. *J. Clean. Prod.* **2020**, *252*, 119389.

(13) Khatab, S.; Leijs, M. J.; van Buul, G.; Haeck, J.; Kops, N.; Nieboer, M.; Bos, P. K.; Verhaar, J. A. N.; Bernsen, M.; van Osch, G. J. V. M.; van Osch, G. J. MSC encapsulation in alginate microcapsules prolongs survival after intra-articular injection, a longitudinal in vivo cell and bead integrity tracking study. *Cell Biol. Toxicol.* **2020**, *36*, 553−570.

(14) Wiśniewska, A. B.; Tomaszewski, M.; Hellal, M. S.; Buczyńska, A. Z. Effect of biomass immobilization and reduced graphene oxide

https://doi.org/10.1021/acsomega.1c04469
ACS Omega 2022, 7, 5646−5656

on the microbial community changes and nitrogen removal at low temperatures. *Sci. Rep.* **2021**, *11*, 1−12.
(15) Wang, B.; Wan, Y.; Zheng, Y.; Lee, X.; Liu, T.; Yu, Z.; Huang, J.; Ok, Y. S.; Chen, J.; Gao, B. Alginate-based composites for environmental applications: a critical review. *Crit. Rev. Environ. Sci. Technol.* **2018**, *49*, 318−356.
(16) Hecht, H.; Srebnik, S. Structural characterization of sodium alginate and calcium alginate. *Biomacromolecules* **2016**, *17*, 2160−2167.
(17) Schild, H. G. Poly (N-isopropylacrylamide): experiment, theory and application. *Prog. Polym. Sci.* **1992**, *17*, 163−249.
(18) Ziółkowski, B.; Florea, L.; Theobald, J.; Benito-Lopez, F.; Diamond, D. Porous self-protonating spiropyran-based NIPAAm gels with improved reswelling kinetics. *J. Mater. Sci.* **2016**, *51*, 1392−1399.
(19) Brahima, S.; Boztepe, C.; Kunkul, A.; Yuceer, M. Modeling of drug release behavior of pH and temperature sensitive poly (NIPAAm-co-AAc) IPN hydrogels using response surface methodology and artificial neural networks. *Mater. Sci. Eng., C* **2017**, *75*, 425−432.
(20) Fathi, M.; Entezami, A. A.; Pashaei-Asl, R. Swelling/deswelling, thermal, and rheological behavior of PVA-g-NIPAAm nanohydrogels prepared by a facile free-radical polymerization method. *J. Polym. Res.* **2013**, *20*, 1−11.
(21) Jankaew, R.; Rodkate, N.; Lamlertthon, S.; Rutnakornpituk, B.; Wichai, U.; Ross, G.; Rutnakornpituk, M. "Smart" carboxymethylchitosan hydrogels crosslinked with poly (N-isopropylacrylamide) and poly (acrylic acid) for controlled drug release. *Polym. Test.* **2015**, *42*, 26−36.
(22) Mahida, V. P.; Patel, M. P. Superabsorbent amphoteric nanohydrogels: Synthesis, characterization and dyes adsorption studies. *Chin. Chem. Lett.* **2016**, *27*, 471−474.
(23) Fathi, M.; Entezami, A. A.; Arami, S.; Rashidi, M.-R. Preparation of N-isopropylacrylamide/itaconic acid magnetic nanohydrogels by modified starch as a crosslinker for anticancer drug carriers. *Int. J. Polym. Mater. Polym. Biomater.* **2015**, *64*, 541−549.
(24) Tang, S.; Floy, M.; Bhandari, R.; Dziubla, T.; Hilt, J. Development of novel N-isopropylacrylamide (NIPAAm) based hydrogels with varying content of chrysin multiacrylate. *Gels* **2017**, *3*, 40.
(25) Tang, S.; Floy, M.; Bhandari, R.; Sunkara, M.; Morris, A. J.; Dziubla, T. D.; Hilt, J. Z. Synthesis and characterization of thermoresponsive hydrogels based on N-isopropylacrylamide crosslinked with 4, 4′-dihydroxybiphenyl diacrylate. *ACS Omega* **2017**, *2*, 8723−8729.
(26) Dodero, A.; Pianella, L.; Vicini, S.; Alloisio, M.; Ottonelli, M.; Castellano, M. Alginate-based hydrogels prepared via ionic gelation: An experimental design approach to predict the crosslinking degree. *Eur. Polym. J.* **2019**, *118*, 586−594.
(27) Patel, M. A.; AbouGhaly, M. H. H.; Schryer-Praga, J. V.; Chadwick, K. The effect of ionotropic gelation residence time on alginate cross-linking and properties. *Carbohydr. Polym.* **2017**, *155*, 362−371.
(28) Haldar, K.; Chakraborty, S. Effect of liquid pool concentration on chemically reactive drop impact gelation process. *J. Colloid Interface Sci.* **2018**, *528*, 156−165.
(29) Song, B.; Liang, H.; Sun, R.; Peng, P.; Jiang, Y.; She, D. Hydrogel synthesis based on lignin/sodium alginate and application in agriculture. *Int. J. Biol. Macromol.* **2020**, *144*, 219−230.
(30) Song, Y.-c.; Tong, W.-j.; Gao, C.-y. Regulation of Free Carboxylate Groups of Alginate Microspheres with Nacl Solution and Its Effect in Doxorubicin Loading and Release. *Gaofenzi Xuebao* **2012**, *012*, 771−777.
(31) Rudke, A. R.; Heleno, S. A.; Fernandes, I. P.; Prieto, M. A.; Gonçalves, O. H.; Rodrigues, A. E.; Ferreira, I. C. F. R.; Barreiro, M. F. Microencapsulation of ergosterol and Agaricus bisporus L. extracts by complex coacervation using whey protein and chitosan: Optimization study using response surface methodology. *LWT—Food Sci. Technol.* **2019**, *103*, 228−237.
(32) Jiang, Z. Q. Preparation and Characterization of Calcium Microcapsules with Intelligent Double Response Alginate. M.D. Dissertation; Xi'an University of Science and Technology: Xi'an, China, 2018. https://kns.cnki.net/KCMS/detail/detail.aspx?dbname=CMFD201901&filename=1018882911.nh (accessed Dec 16, 2018).
(33) Gholamian, S.; Nourani, M.; Bakhshi, N. Formation and characterization of calcium alginate hydrogel beads filled with cumin seeds essential oil. *Food Chem.* **2021**, *338*, 128143.
(34) Najafi-Soulari, S.; Shekarchizadeh, H.; Kadivar, M. Encapsulation optimization of lemon balm antioxidants in calcium alginate hydrogels. *J. Biomater. Sci., Polym. Ed.* **2016**, *27*, 1631−1644.
(35) Wang, J.; Zhang, B. H.; Cui, X. C.; Kong, X. P. Preparation of temperature and pH-sensitive carboxymethyl chitosan/sodium alginate hydrogel microsphere. *Yingyong Huagong* **2015**, *44*, 1464−1467.
(36) Chalanqui, M. J.; Pentlavalli, S.; McCrudden, C.; Chambers, P.; Ziminska, M.; Dunne, N.; McCarthy, H. O. Influence of alginate backbone on efficacy of thermo-responsive alginate-g-P(NIPAAm) hydrogel as a vehicle for sustained and controlled gene delivery. *Mater. Sci. Eng., C* **2019**, *95*, 409−421.
(37) Krušić, M. K.; Filipović, J. Copolymer hydrogels based on N-isopropylacrylamide and itaconic acid. *Polymer* **2006**, *47*, 148−155.
(38) Taşdelen, B.; Çifçi, D. . İ.; Meriç, S. Preparation of N-isopropylacrylamide/itaconic acid/Pumice highly swollen composite hydrogels to explore their removal capacity of methylene blue. *Colloids Surf., A* **2017**, *519*, 245−253.
(39) Yao, G.; Bi, W.; Liu, H. pH-responsive magnetic graphene oxide/poly (NVI-co-AA) hydrogel as an easily recyclable adsorbent for cationic and anionic dyes. *Colloids Surf., A* **2020**, *588*, 124393.
(40) Alvarado, A. G.; Cortés, J.; Pérez-Carrillo, L. A.; Rabelero, M.; Arellano, J.; Sánchez-Díaz, J. C.; Puig, J. E.; Arellano, M. Temperature and pH-Responsive Polyacrylamide/Poly (Acrylic Acid) Interpenetrating Polymer Network Nanoparticles. *J. Macromol. Sci., Part B: Phys.* **2016**, *55*, 1086−1098.
(41) Wang, P.; He, Y.; Ding, J.; Wang, W.; Sheng, H.; Wei, Z.; Huang, M.; Zhang, H. Feasibility of iron scraps for enhancing nitrification of domestic wastewater at low temperatures. *Environ. Sci. Pollut. Res.* **2021**, *28*, 26819−26827.
(42) Zhang, Y.; Yu, Z.; Hu, Y.; Song, C.; Li, F.; He, W.; Wang, X.; Li, Z.; Lin, H. Immobilization of nitrifying bacteria in magnetic PVA−SA-diatomite carrier for efficient removal of NH4+-N from effluents. *Environ. Technol. Innovat.* **2021**, *22*, 101407.
(43) Meng, J.; Li, J.; Li, J.; Nan, J.; Deng, K.; Antwi, P. Effect of temperature on nitrogen removal and biological mechanism in an up-flow microaerobic sludge reactor treating wastewater rich in ammonium and lack in carbon source. *Chemosphere* **2019**, *216*, 186−194.
(44) Du, Q. P.; Chen, Z. M.; Li, Y. X.; Li, L.; Ling, J. Y.; Xu, Y. B. Effects of Activated Carbon in Sodium Alginate and Polyvinylacohol Immobilization Pellets of Penicillium sp. on Chlorobenzene Removal. *Guangdong Gongye Daxue Xuebao* **2017**, *34*, 22−26.
(45) Ociński, D.; Jacukowicz-Sobala, I.; Kociołek-Balawejder, E. Alginate beads containing water treatment residuals for arsenic removal from water—formation and adsorption studies. *Environ. Sci. Pollut. Res.* **2016**, *23*, 24527−24539.
(46) Godiya, C. B.; Xiao, Y.; Lu, X. Amine functionalized sodium alginate hydrogel for efficient and rapid removal of methyl blue in water. *Int. J. Biol. Macromol.* **2020**, *144*, 671−681.
(47) Olad, A.; Pourkhiyabi, M.; Gharekhani, H.; Doustdar, F. Semi-IPN superabsorbent nanocomposite based on sodium alginate and montmorillonite: Reaction parameters and swelling characteristics. *Carbohydr. Polym.* **2018**, *190*, 295−306.
(48) Choi, D.; Lee, D.; Yun, W.; Jung, J. Addition of a foaming agent to improve N2 gas permeability of PVA/alginate carriers for deammonification process. *Int. J. Hydrogen Energy* **2017**, *42*, 27812−27819.
(49) Gong, W.; Fan, Y.; Xie, B.; Tang, X.; Guo, T.; Luo, L.; Liang, H. Immobilizing Microcystis aeruginosa and powdered activated

https://doi.org/10.1021/acsomega.1c04469
ACS Omega 2022, 7, 5646−5656

carbon for the anaerobic digestate effluent treatment. *Chemosphere* **2020**, *244*, 125420.
(50) Sun, L.; Wang, J.; Liang, J.; Li, G. Boric acid cross-linked 3D polyvinyl alcohol gel beads by NaOH-titration method as a suitable biomass immobilization matrix. *J. Polym. Environ.* **2020**, *28*, 532−541.
(51) Li, Z.; Wu, W.; Jiang, W.; Zhang, L.; Li, Y.; Tan, Y.; Chen, S.; Lv, M.; Luo, F.; Luo, T.; Wei, G. Preparation and regeneration of a thermo-sensitive adsorbent material: methyl cellulose/calcium alginate beads (MC/CABs). *Polym. Bull. (Heidelberg, Ger.)* **2020**, *77*, 1707−1728.
(52) Wang, J.; Fan, Y. C.; Chen, Y. P. Nitrogen removal performance and characteristics of gel beads immobilized anammox bacteria under different PVA: SA ratios. *Water Environ. Res.* **2021**, *93*, 1627.
(53) Zhang, Y.; Hui, B.; Ye, L. Reactive toughening of polyvinyl alcohol hydrogel and its wastewater treatment performance by immobilization of microorganisms. *RSC Adv.* **2015**, *5*, 91414−91422.
(54) You, Z.; Xu, H.; Shah, K. J.; Tao, J.; Cai, D. Enhance Pyrene Degradation of Sodium Alginate Embedding Immobilization by Adding PAC. *CET* **2020**, *81*, 19−24.

https://doi.org/10.1021/acsomega.1c04469
ACS Omega 2022, 7, 5646−5656